The tyrosine phosphatase SHP2 regulates recovery of endothelial adherens junctions through control of β-catenin phosphorylation

Ilse Timmerman[a], Mark Hoogenboezem[a], Anton M. Bennett[b], Dirk Geerts[c], Peter L. Hordijk[a], and Jaap D. van Buul[a]

[a]Department of Molecular Cell Biology, Sanquin Research and Landsteiner Laboratory, Academic Medical Center, University of Amsterdam, 1066 CX Amsterdam, Netherlands; [b]Department of Pharmacology, Yale University School of Medicine, New Haven, CT 06520; [c]Department of Pediatric Oncology/Hematology, Erasmus University Medical Center, 3015 GE Rotterdam, Netherlands

ABSTRACT **Impaired endothelial barrier function results in a persistent increase in endothelial permeability and vascular leakage. Repair of a dysfunctional endothelial barrier requires controlled restoration of adherens junctions, comprising vascular endothelial (VE)-cadherin and associated β-, γ-, α-, and p120-catenins. Little is known about the mechanisms by which recovery of VE-cadherin–mediated cell–cell junctions is regulated. Using the inflammatory mediator thrombin, we demonstrate an important role for the Src homology 2-domain containing tyrosine phosphatase (SHP2) in mediating recovery of the VE-cadherin–controlled endothelial barrier. Using SHP2 substrate-trapping mutants and an in vitro phosphatase activity assay, we validate β-catenin as a bona fide SHP2 substrate. SHP2 silencing and SHP2 inhibition both result in delayed recovery of endothelial barrier function after thrombin stimulation. Moreover, on thrombin challenge, we find prolonged elevation in tyrosine phosphorylation levels of VE-cadherin–associated β-catenin in SHP2-depleted cells. No disassembly of the VE-cadherin complex is observed throughout the thrombin response. Using fluorescence recovery after photobleaching, we show that loss of SHP2 reduces the mobility of VE-cadherin at recovered cell–cell junctions. In conclusion, our data show that the SHP2 phosphatase plays an important role in the recovery of disrupted endothelial cell–cell junctions by dephosphorylating VE-cadherin–associated β-catenin and promoting the mobility of VE-cadherin at the plasma membrane.**

Monitoring Editor
Mark H. Ginsberg
University of California, San Diego

Received: Jan 20, 2012
Revised: Jul 13, 2012
Accepted: Aug 29, 2012

INTRODUCTION

The endothelium lines the vessel wall and serves as a selective barrier controlling the passage of fluids, macromolecules, and leukocytes from blood to the underlying tissues. Loss of the specific barrier function leads to a persistent increase in endothelial permeability and edema, which can result in chronic inflammation and organ dysfunction (Weis and Cheresh, 2005). Endothelial permeability is controlled in part by the coordinated opening and closing of intercellular junctions (Muller, 2001; Dejana *et al.*, 2008).The adherens junction complex, comprising vascular endothelial (VE)-cadherin and catenins, is of central importance for the initiation and stabilization of these cell–cell contacts (Breviario *et al.*, 1995; Matsuyoshi *et al.*, 1997; Crosby *et al.*, 2005).

VE-cadherin mediates homophilic, calcium-dependent adhesion between adjacent cells (Breviario *et al.*, 1995). VE-cadherin also binds to many cytoplasmic proteins, particularly members of the catenin family, which contribute to the anchoring of the cadherin to the actin cytoskeleton (Kemler, 1993). The cytoplasmic tail of VE-cadherin contains a proximal binding site for p120-catenin and a distal binding site for β-catenin and plakoglobin (also called

This article was published online ahead of print in MBoC in Press (http://www.molbiolcell.org/cgi/doi/10.1091/mbc.E12-01-0038) on September 5, 2012.

Address correspondence to: Jaap D. van Buul (j.vanbuul@sanquin.nl).

Abbreviations used: ECIS, electric cell-substrate impedance sensing; FRAP, fluorescence recovery after photobleaching; HUVEC, human umbilical vein endothelial cell; PTP, protein tyrosine phosphatase; SHP2, Src homology 2-domain containing tyrosine phosphatase; TER, transendothelial electrical resistance; VE-cadherin, vascular endothelial cadherin.

γ-catenin). Both β-catenin and plakoglobin are linked to α-catenin, which further interacts with actin-binding proteins, thereby providing a physical link to the actin cytoskeleton (Vincent *et al.*, 2004). p120-Catenin has been reported to influence cadherin function by a variety of mechanisms, including plasma membrane stability, recycling, and cell surface targeting (Davis *et al.*, 2003; Xiao *et al.*, 2003, 2005, 2007). Various studies have demonstrated that binding of these catenins is important for the optimal adhesive function of VE-cadherin (Kemler, 1993; Navarro *et al.*, 1995; Ferber *et al.*, 2002).

Tyrosine phosphorylation of the VE-cadherin complex has often been proposed as a mechanism that controls the integrity of the adherens junction (Daniel and Reynolds, 1997). Several studies have shown a correlation between phosphorylation of the cadherin–catenin complex and increased vascular permeability in response to inflammatory mediators and growth factors (Rabiet *et al.*, 1996; Esser *et al.*, 1998; Andriopoulou *et al.*, 1999; Konstantoulaki *et al.*, 2003; Hudry-Clergeon *et al.*, 2005; Angelini *et al.*, 2006; Monaghan-Benson and Burridge, 2009). Although use of phosphomutants underscored the importance of VE-cadherin tyrosine phosphorylation in the regulation of the endothelial barrier function (Potter *et al.*, 2005; Allingham *et al.*, 2007; Turowski *et al.*, 2008), the consequences of catenin phosphorylation for vascular permeability have been less intensively studied. Nevertheless, data from studies using epithelial cells show that tyrosine phosphorylation of β-catenin is consistently correlated with loss of E-cadherin function (Roura *et al.*, 1999; Lilien and Balsamo, 2005; Winter *et al.*, 2008), indicating that β-catenin may also play an important role in the regulation of VE-cadherin adhesiveness. The regulation of tyrosine phosphorylation results from a competing balance of protein tyrosine kinase and protein tyrosine phosphatase (PTP) activity. Whereas most studies in this area are focused on the tyrosine kinases and their targets within cell–cell junctions, the critical role of PTPs that act on junctional proteins becomes more profound. Several PTPs have been shown to associate with components of the VE-cadherin complex, maintaining low levels of tyrosine phosphorylation and thereby promoting endothelial barrier function. VE-cadherin–associated PTPs include PTP-μ, VE-PTP, PTP1B, and Src homology 2-domain containing tyrosine phosphatase (SHP2; Ukropec *et al.*, 2000; Nawroth *et al.*, 2002; Sui *et al.*, 2005; Nakamura *et al.*, 2008; Nottebaum *et al.*, 2008).

SHP2 (previously called SH-PTP2, PT-P2C, PTP1D, or Syp) is a ubiquitously expressed nonreceptor PTP containing two N-terminal tandem SH2 domains followed by a catalytic phosphatase (PTP) domain and a C-terminal tail with two tyrosine residues (Neel *et al.*, 2003). Ukropec *et al.* (2000) reported that SHP2 associates with VE-cadherin through β-catenin using far-Western blotting. In addition, they showed that thrombin treatment of endothelial cells induced SHP2 tyrosine phosphorylation. In the present study, we use the inflammatory mediator thrombin to study the mechanism by which the reassembly of VE-cadherin–mediated cell–cell junctions is regulated. We show that SHP2 controls the recovery of endothelial barrier function by dephosphorylating β-catenin and promoting the mobility of VE-cadherin at the plasma membrane.

RESULTS

The thrombin-induced decrease in endothelial monolayer resistance is accompanied by increased tyrosine phosphorylation of VE-cadherin–associated β-catenin

To study the process of endothelial cell–cell junction recovery, we used the inflammatory mediator thrombin. Using electrical cell-substrate impedance sensing (ECIS), we observed that thrombin induced a decrease in transendothelial electrical resistance (TER) within 5 min (Figure 1A). The reduction in TER was maximal after 30 min but was reversible and restored within 3 h (Figure 1A). Confocal microscopy analysis showed that the thrombin-induced decrease in TER is accompanied by transiently enhanced tyrosine phosphorylation of junctional proteins (Figure 1B). Western blot analysis of a VE-cadherin immunoprecipitation revealed that specifically VE-cadherin–associated β-catenin was phosphorylated on tyrosine residues after 5 min of thrombin treatment (Figure 1C). In addition, increased tyrosine phosphorylation was observed when β-catenin was immunoprecipitated (Figure 1D). The rapid increase in tyrosine phosphorylation of VE-cadherin–associated β-catenin was confirmed by sequential immunoprecipitation in which tyrosine phosphorylated proteins were immunoprecipitated from a VE-cadherin immunocomplex and analyzed for the presence of β-catenin (Figure 1E).

Tyrosine phosphorylation of VE-cadherin and the catenins has often been reported to lead to disassembly of the complex, resulting in uncoupling of VE-cadherin from the actin cytoskeleton (Rabiet *et al.*, 1996; Potter *et al.*, 2005; Monaghan-Benson and Burridge, 2009). However, the thrombin-induced phosphorylation events did not block the coimmunoprecipitation of VE-cadherin with p120-, α-, and β-catenin (Figure 1C). Moreover, no change was found in the colocalization of adherens junction proteins at the cell–cell junctions after thrombin administration (Supplemental Figure S1). Taken together, these results show that the VE-cadherin complex remained intact upon thrombin stimulation. Of interest, tyrosine phosphorylation levels are only briefly increased upon thrombin treatment. Prolonged analysis of tyrosine phosphorylation of β-catenin showed a drop in tyrosine phosphorylation levels at time points that reflected the recovery of the endothelial monolayer (Figure 1, C–E). Thus thrombin rapidly disrupted cell–cell junctions and transiently increased tyrosine phosphorylation of VE-cadherin–associated β-catenin.

SHP2 dephosphorylates VE-cadherin–associated β-catenin in response to thrombin

Dephosphorylation of β-catenin during the recovery phase of the thrombin response can be attributed to elevated tyrosine phosphatase activity. A possible candidate is the protein tyrosine phosphatase SHP2, which has been shown to bind β-catenin by far-Western blotting (Ukropec *et al.*, 2000). Confocal microscopy imaging revealed the presence of endogenous SHP2 at endothelial cell–cell junctions (Figure 2A). Tyrosine phosphorylation of SHP2 was previously shown to be important for its signaling functions. We found that thrombin induced an increase in tyrosine phosphorylation of SHP2, especially after 30–60 min (Figure 2B and Supplemental Figure S2A). More specifically, thrombin stimulation resulted in phosphorylation of SHP2 at tyrosine residue 542 (Figure 2B), which has been described as promoting SHP2 activity (Lu *et al.*, 2001; Araki *et al.*, 2003). To further test whether thrombin stimulation results in activation of SHP2, we measured in vitro PTP activity. SHP2 was immunoprecipitated from lysates of thrombin-treated endothelial cells and incubated with phosphopeptides. Phosphate release into the supernatant was detected by addition of Malachite green. SHP2 activity levels were approximately twofold higher when endothelial cells were stimulated for 30 or 45 min with thrombin, whereas no effect was observed after 5 min (Figure 2C). Similar to SHP2, phosphorylation of Src kinase was increased after 30–45 min of thrombin stimulation, specifically at tyrosine residue 418, indicating increased Src kinase activity (Figure 2D). Therefore we tested whether inhibition of Src kinases affected thrombin-induced SHP2 activation. Src-family kinase inhibition by both PP2 and SU6656 prevented the increase in SHP2 activity upon thrombin treatment

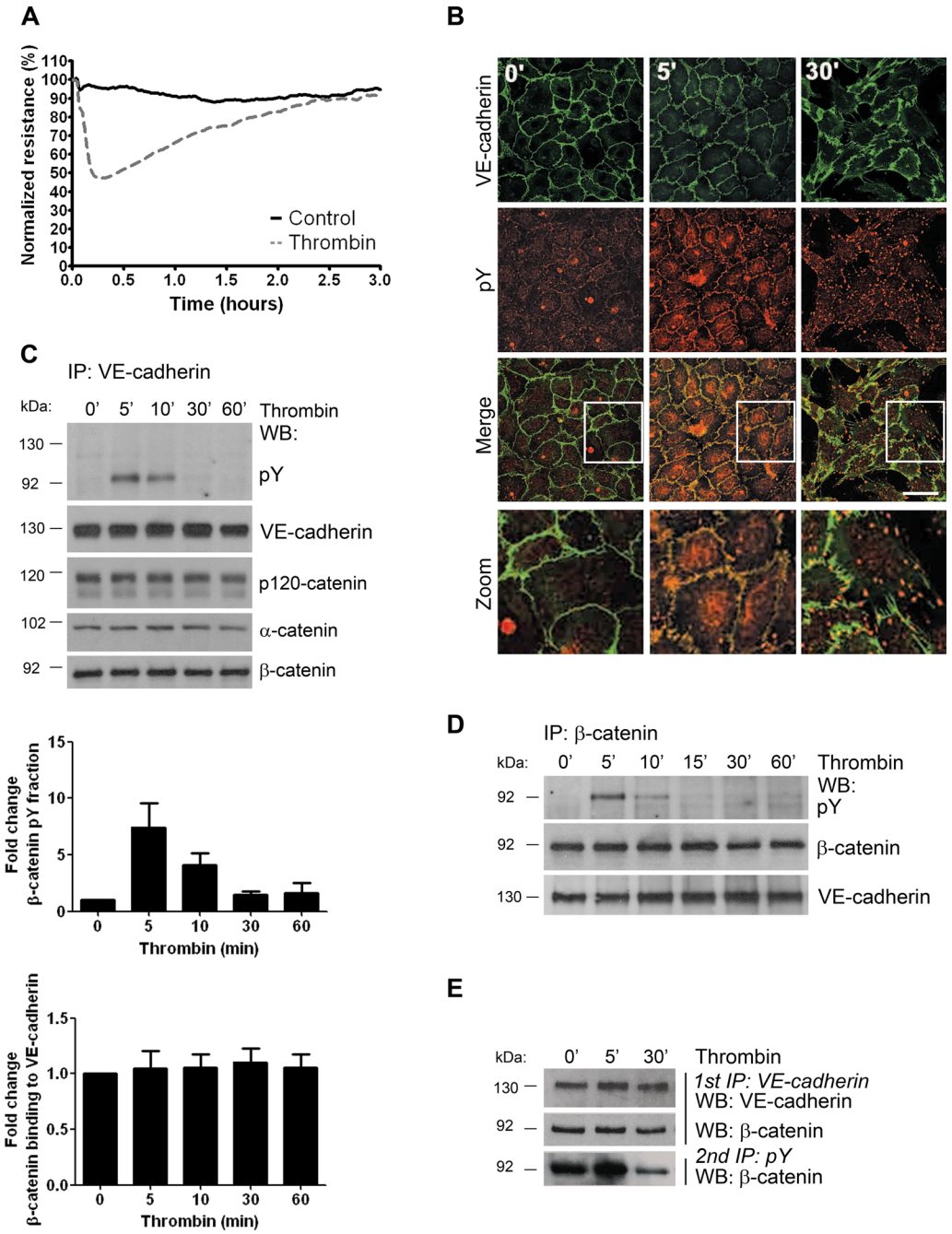

FIGURE 1: Thrombin induces a transient drop in the TER of endothelial monolayers and transiently increases tyrosine phosphorylation of VE-cadherin–associated β-catenin. (A) HUVECs were cultured to confluency on FN-coated electrode arrays. At time point 0, cells were incubated with (dashed line) or without (solid line) thrombin and electrical resistance was monitored in time by ECIS. Thrombin rapidly decreased the resistance of the endothelial monolayer, which was restored after 2–3 h. (B) HUVECs were cultured on FN-coated glass covers, grown to confluency, and stimulated with thrombin for 5 or 30 min, as indicated. Immunostaining for VE-cadherin (green) and phosphotyrosine (pY, red) shows colocalization at cell–cell junctions after 5 min of thrombin stimulation (merged image, colocalization appears in yellow). Bar, 20 μm. (C) VE-cadherin was immunoprecipitated from control or thrombin-treated HUVECs, and phosphorylation levels were determined by Western blotting (WB) with an anti-phosphotyrosine antibody. Top, thrombin induces an increase in tyrosine phosphorylation (pY) of a ~92-kDa cadherin-associating protein, likely β-catenin. Bottom, equal levels of VE-cadherin and catenins were immunoprecipitated. Top bar graph, fold increase in tyrosine phosphorylation relative to the levels of VE-cadherin–associating β-catenin. Bottom bar graph, relative binding of β-catenin to VE-cadherin during thrombin stimulation. Results are means ± SD of four independent experiments. (D) β-Catenin was immunoprecipitated from control or thrombin-treated HUVEC, and phosphorylation levels were determined by Western blotting. (E) HUVECs were stimulated with thrombin and lysed, and IP for VE-cadherin was performed (1st IP). The washed pellet was incubated with lysis buffer containing 1% SDS, and the supernatant was recovered and subjected to a second IP using pY antibodies to precipitate tyrosine-phosphorylated proteins from the dissociated VE-cadherin complex (2nd IP; pY). Blot shows increased tyrosine phosphorylation of VE-cadherin–bound β-catenin after 5 min of thrombin treatment, which was reduced after 30 min.

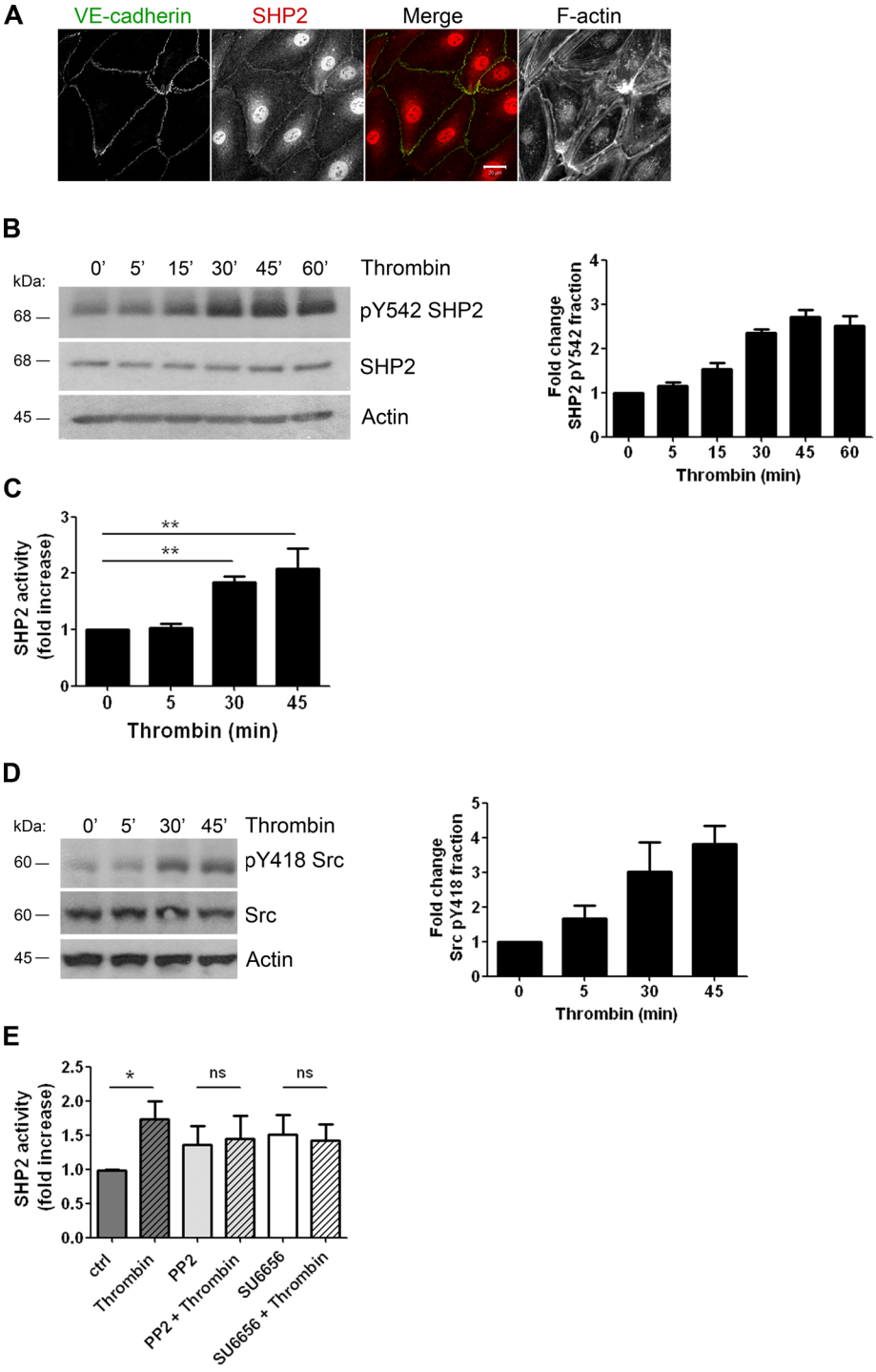

FIGURE 2: Thrombin induces Src-mediated activation of SHP2. (A) HUVECs were cultured on FN-coated glass covers, grown to confluency, and stained for SHP2 in red, VE-cadherin in green, and F-actin. SHP2 partially localizes at cell–cell contacts. Bar, 20 μm. (B) HUVECs were stimulated with thrombin as indicated and lysed, and SHP2 phosphorylation at tyrosine residue 542 was analyzed using a phosphospecific antibody. Bar graph at the right, fold increase in SHP2 tyrosine phosphorylation after thrombin stimulation. (C) SHP2 was immunoprecipitated from thrombin-treated HUVEC and subjected to a tyrosine phosphatase activity assay as described in *Materials and Methods*. (D) HUVECs were stimulated with thrombin and lysed, and Src-family kinase phosphorylation at tyrosine residue 418 was analyzed using a phosphospecific antibody. Bar graph, fold increase in phosphorylation of Src at pY418 upon thrombin treatment. (E) HUVECs were pretreated with dimethyl sulfoxide or the Src-family kinase inhibitor PP2 or SU6656 and stimulated with thrombin for 45 min. PP2 and SU6656 inhibited the thrombin-induced increase in SHP2 activity. Data are mean ± SEM of three independent experiments. ns, not significant; $*p < 0.05$, $**p < 0.01$.

(Figure 2E). Thus SHP2 activity increases after 30–45 min of thrombin stimulation, which is dependent on Src kinase.

To study whether β-catenin is a SHP2 substrate, we sought to establish whether catalytic inactive substrate-trapping SHP2 mutants complexed with β-catenin. To accomplish this, we treated Cos-7 cells with vanadate to inhibit tyrosine phosphatases and subjected lysates to affinity precipitation with either glutathione *S*-transferase (GST)–SHP2 PTP domain (GST-SHP2–wild type [WT]) or the substrate-trapping mutant (GST-SHP2-DA). We found that β-catenin bound to GST-SHP2-DA to a greater extent than to GST-SHP2-WT (Figure 3A). To demonstrate that SHP2 substrate-trapping interactions are not limited to in vitro conditions, we tested whether the substrate-trapping mutants of SHP2 complexed with β-catenin in a cellular context. Cos-7 cells were transfected with the vector control, pIRES–green fluorescent protein (GFP) myc-tagged wild-type SHP2 (SHP2-WT), or the substrate-trapping mutants of SHP2 (SHP2-DA and SHP2-CS). SHP2 was immunoprecipitated from lysates with anti-myc antibodies and immunoblotted for the presence of β-catenin. We found that SHP2-DA and SHP2-CS both coprecipitated with β-catenin, whereas complex formation was less evident with SHP2-WT (Figure 3B). Of importance, the interaction of β-catenin with SHP2-CS was disrupted by vanadate, an active-site PTP inhibitor (Huyer *et al.*, 1997). Taken together, these data demonstrate that SHP2 forms an enzyme–substrate complex with β-catenin. To further characterize β-catenin as a substrate for SHP2, we tested whether SHP2 is able to dephosphorylate β-catenin in vitro. SHP2 was immunoprecipitated from lysates of thrombin-stimulated endothelial cells, incubated with tyrosine-phosphorylated β-catenin, which was immunoprecipitated from vanadate-treated cells, and subjected to a tyrosine phosphatase activity assay. Addition of tyrosine-phosphorylated β-catenin to the SHP2 immunocomplex resulted in an increase in the amount of released phosphate (Figure 3C). This increase in phosphate release was less evident when β-catenin was immunoprecipitated from untreated cells or when SHP2 was immunoprecipitated from vanadate-treated cells, which inhibits SHP2 function. These data indicate that SHP2 is capable of dephosphorylating β-catenin.

To examine the involvement of SHP2 in dephosphorylation of VE-cadherin–associated β-catenin after thrombin stimulation, we used small interfering RNA (siRNA) to reduce SHP2 expression in endothelial cells.

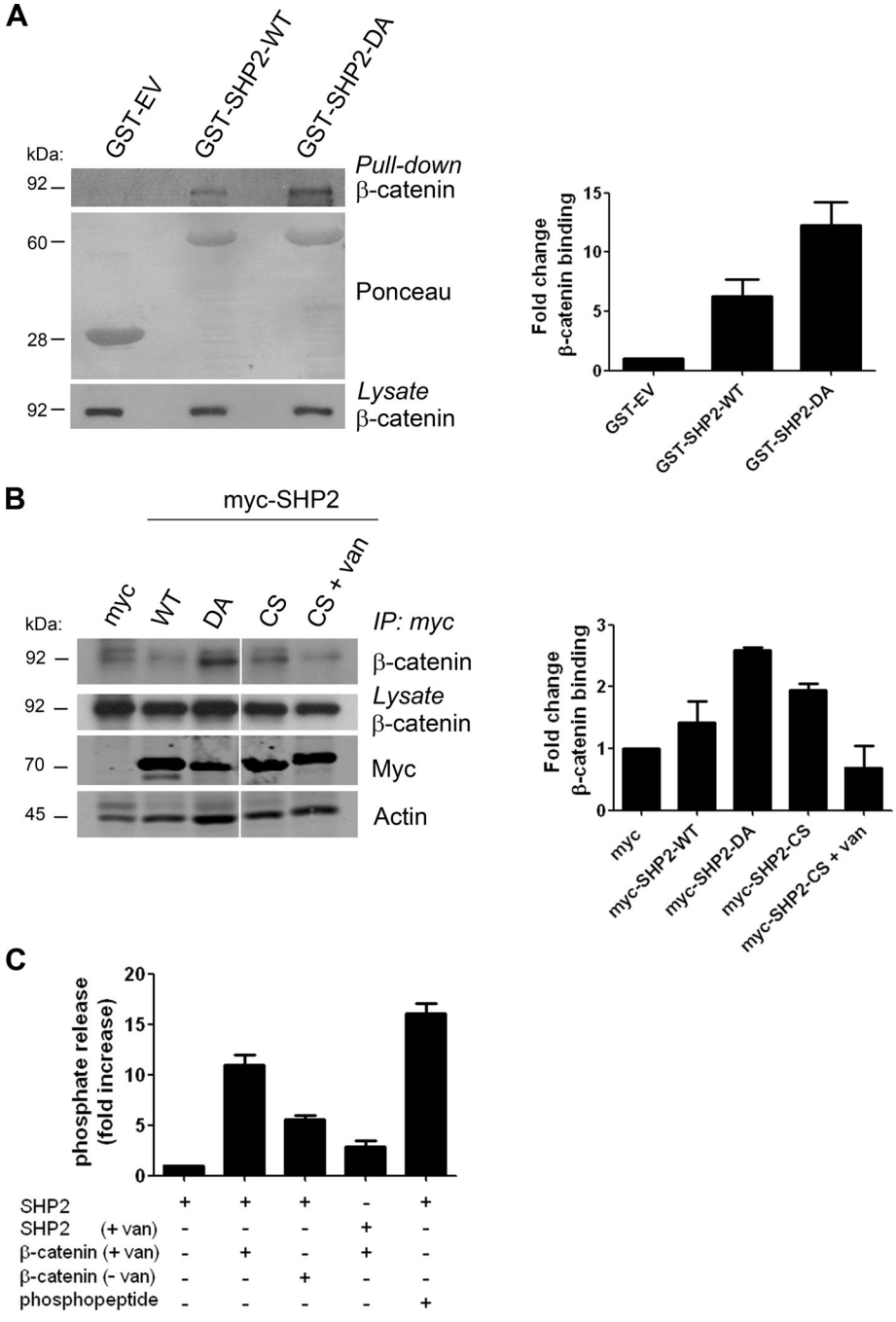

FIGURE 3: In vitro dephosphorylation and substrate trapping of β-catenin by SHP2. (A) Lysates prepared from Cos-7 cells were incubated with GST, GST-fusion protein of SHP2 PTP domain (GST-SHP2-WT), or the substrate-trapping mutant (GST-SHP2-DA). GST affinity-purified complexes were immunoblotted for β-catenin. Bar graph, the relative binding of β-catenin to SHP2-WT and SHP2-DA. (B) Cos-7 cells were transfected with myc vector, myc-SHP2-WT, or the myc-tagged SHP2 substrate-trapping mutant DA or CS. Lysates were subjected to immunoprecipitation with anti-myc antibodies, and immune complexes were immunoblotted for β-catenin. The myc-SHP2-CS immunocomplexes were also pretreated with vanadate (van; 10 mM). Bar graph, the relative binding of β-catenin to myc-SHP2-WT, myc-SHP2-DA, and myc-SHP2-CS. (C) SHP2 was immunoprecipitated from lysates of thrombin-stimulated HUVEC, incubated with immunoprecipitated β-catenin, and subjected to a tyrosine phosphatase activity assay as described in *Materials and Methods*. β-Catenin was immunoprecipitated from untreated (–van) or vanadate-treated (+van) Cos-7 cells, preventing protein dephosphorylation. As a positive control, phosphopeptides were incubated with the SHP2 immunocomplex. As a negative control, SHP2 immunocomplexes from vanadate-treated cells were included. Bar graph, fold increase in phosphate release.

VE-cadherin was immunoprecipitated from lysates of thrombin-treated endothelial cells that were transfected with siRNA against SHP2 or control siRNA. Subsequently the immunoprecipitates were processed for phosphotyrosine immunoblotting. In the control endothelial monolayers, an increase in tyrosine phosphorylation of the cadherin complex was observed after 5 min of thrombin stimulation, which declined at 30 min (Figure 4A). Of interest, SHP2-silenced endothelial monolayers showed prolonged and elevated tyrosine phosphorylation upon thrombin stimulation of a cadherin-associating protein of ~92 kDa, suggesting that phosphorylation of β-catenin was modulated. Similarly, prolonged tyrosine phosphorylation was observed upon SHP2 inhibition, using the compound PHPS1, which acts as a competitive and selective inhibitor of SHP2 (Supplemental Figure S2, B and C; Hellmuth *et al.*, 2008). To test whether tyrosine phosphorylation of VE-cadherin–bound β-catenin indeed was increased, we performed a sequential immunoprecipitation in which we first immunoprecipitated VE-cadherin, followed by a phosphotyrosine immunoprecipitation. The Western blot was analyzed for the presence of β-catenin and showed a marked increase in its tyrosine phosphorylation at 30 min after thrombin stimulation in SHP2-depleted cells compared with control endothelial cells (Figure 4B). Reconstitution of SHP2 in SHP2-depleted cells, by infecting siRNA-treated endothelial cells with adenovirus containing pIRES-GFP-SHP2, reversed the prolonged tyrosine phosphorylation of β-catenin that was measured in SHP2-depleted cells (Figure 4C). In contrast, expression of a catalytically inactive mutant of SHP2 (ΔP) failed to rescue β-catenin dephosphorylation in SHP2-depleted cells. These data indicate that SHP2 regulates the dephosphorylation of VE-cadherin–bound β-catenin upon stimulation with thrombin.

SHP2 is required for efficient recovery of cell–cell junctions and for restoration of the endothelial barrier function

On the basis of the kinetics of thrombin-induced SHP2 activation, we tested whether SHP2 contributes to the recovery of the endothelial barrier function. Using ECIS, we determined the effect of SHP2 silencing by siRNA on the electrical resistance of the endothelial monolayer upon thrombin stimulation (Figure 5, A and B). Of interest, SHP2 depletion using siRNA or short hairpin RNA (shRNA) did not affect the thrombin-induced drop in resistance but did delay the

recovery of endothelial monolayer integrity. SHP2 inhibition, using the compound PHPS1, resulted in a similar delay in endothelial barrier recovery after thrombin (Figure 5B). The basal resistance of the endothelial monolayer was unaltered upon SHP2 silencing (Figure 5C), demonstrating that the assembly of endothelial cell–cell junctions during monolayer formation was not impaired. This suggested that SHP2 silencing affects the specific ability of the endothelial cells to re-form cell–cell junctions after endothelial monolayer disruption. Impaired junction reassembly after thrombin stimulation of SHP2-depleted monolayers was also observed using fluorescence microscopy (Figure 5, D and E), as judged from the increased number of intercellular gaps 2 h after thrombin stimulation. To exclude the possibility that the delayed barrier recovery is mainly caused by impaired spreading of SHP2-depleted endothelial cells, we compared spreading of control and SHP2 siRNA- or shRNA-treated cells using ECIS (Figure 5C and Supplemental Figure S3A). In both conditions, that is, control and SHP2 silencing, the electrical resistance increased with a similar rate upon cell spreading. In addition, when analyzed by microscopy, no morphological difference was observed between control and SHP2-depleted endothelial cells upon spreading (Supplemental Figure S3B).

We further wished to determine whether the catalytic activity of SHP2 controls endothelial cell–cell junction recovery. To test this, we first transfected endothelial cells with siRNA against SHP2 or control siRNA, followed after 2 d by infection with adenovirus expressing pIRES-GFP-SHP2-WT or the catalytically inactive ΔP mutant. Again, the basal endothelial monolayer resistance was unaltered when SHP2 function was abrogated, in this case by expressing a catalytically inactive SHP2 mutant (Supplemental Figure S3C). In contrast, the delayed restoration of endothelial monolayer integrity after thrombin treatment in SHP2-depleted cells was partially rescued by reconstitution with SHP2-WT, whereas expression of SHP2-ΔP had no effect (Figure 5F). These data reveal that the PTP domain, and hence the catalytic activity of SHP2, is required to efficiently restore the endothelial barrier. Of interest, Src kinase inhibition, which prevented thrombin-induced SHP2 activation (Figure 2E), also resulted in delayed endothelial barrier recovery upon thrombin challenge (Supplemental Figure S4). This suggests that Src kinases are involved in the SHP2-mediated restoration of thrombin-induced endothelial barrier disruption.

To further study whether the effect of SHP2 on endothelial barrier recovery is dependent on adherens junctions, we combined VE-cadherin and β-catenin silencing with SHP2 inhibition using PHPS1 (Figure 5G). VE-cadherin and β-catenin depletion already compromised endothelial barrier restoration upon thrombin treatment, and no additional effect of SHP2 inhibition was observed. These data suggest that SHP2 promotes endothelial barrier recovery through its direct effect on VE-cadherin–mediated cell–cell junctions.

Besides tyrosine phosphorylation of junctional proteins, thrombin also activates several other intracellular pathways that affect adherens junctions and contribute to endothelial hyperpermeability. Thrombin induced the activation of the small GTPases Rac1, RhoA, and Cdc42 (Figure 6, A–C), which are known to regulate actin cytoskeleton organization. Given that SHP2 has also been implicated in the regulation of Rac1, RhoA, and Cdc42 activity (Schoenwaelder *et al.*, 2000; Lacalle *et al.*, 2002; Kontaridis *et al.*, 2004; Bregeon *et al.*, 2009; Wang *et al.*, 2009), we assessed the contribution of these small GTPases to the SHP2-mediated recovery of endothelial monolayer integrity in response to thrombin. Under control conditions, thrombin stimulation resulted in a biphasic pattern of Rac1 activation, with a maximum after 5 and 75 min, reflecting time points of intercellular junction disruption and junction recovery, respectively (Figure 6A). This pattern was also observed when SHP2 expression was reduced, indicating that Rac1 activation occurs independent of SHP2-regulated endothelial barrier recovery. In addition, thrombin stimulation resulted in a rapid increase in RhoA activation in both control and SHP2-depleted endothelial cells (Figure 6B). After 15 and 45 min of thrombin treatment, RhoA-GTP levels declined to basal levels. This was observed in SHP2-depleted cells as well. Moreover, no significant difference in thrombin-induced Cdc42 activation was observed between control and SHP2-depleted endothelial cells (Figure 6C). Taken together, the findings indicate that SHP2 phosphatase activity is required to efficiently recover the endothelial barrier function after vascular injury, independent of the small GTPases Rac1, RhoA, and Cdc42, but instead through modulating the tyrosine phosphorylation levels of VE-cadherin–bound β-catenin.

SHP2 controls VE-cadherin dynamics in order to recover cell–cell junctions

To further study the mechanism by which SHP2 regulates the restoration of endothelial cell–cell junctions, we assessed whether SHP2 depletion affected the mobility of VE-cadherin in the plasma membrane. To this end, we transduced endothelial cells with adenovirus encoding GFP-tagged VE-cadherin and used fluorescence recovery after photobleaching (FRAP) analysis to study the dynamics of VE-cadherin–GFP. We first tested whether nonselective inhibition of protein tyrosine phosphatase (PTP) activity using vanadate affected VE-cadherin dynamics. Treatment of endothelial cells with vanadate rapidly resulted in a disruption of intercellular junctions and increased tyrosine phosphorylation of β-catenin and VE-cadherin within 15 min (Figure 7A and Supplemental Figure S5, A and B). In line with other studies (Lampugnani *et al.*, 1997; Young *et al.*, 2003), and similar to our findings with thrombin-treated cells, the vanadate-induced increase in tyrosine phosphorylation of VE-cadherin and β-catenin did not result in disassembly of the VE-cadherin complex (Figure 7A). However, FRAP analysis showed that vanadate-mediated PTP inhibition resulted in reduced VE-cadherin mobility (Figure 7B). Vanadate treatment reduced the mobile fraction of VE-cadherin–GFP from 57.5% (±1.6) to 39.4% (±1.4) (Figure 7C).

Next we determined the effect of SHP2 on VE-cadherin motility specifically. FRAP analysis of VE-cadherin–GFP revealed no difference in the fluorescence recovery between SHP2 siRNA–treated cells and control cells under baseline conditions (Figure 7D). However, when endothelial cells were challenged with thrombin and recovered junctions were analyzed by FRAP, the mobility of VE-cadherin was reduced in SHP2-depleted cells (Figure 7D and Supplemental Figure S6). Detailed analysis of the data showed that SHP2 silencing significantly reduced the mobile fraction of VE-cadherin–GFP from 54.8% (±0.9) to 36.3% (±0.5; Figure 7E). The findings indicate that tyrosine phosphorylation affected VE-cadherin dynamics and imply that SHP2 controls the recovery of cell–cell junctions by promoting the mobility of VE-cadherin in the plasma membrane.

DISCUSSION

Repair of the endothelial barrier after vascular injury is a crucial process for maintaining vascular homeostasis. To address the process of cell–cell junction recovery, we used the model of thrombin-induced PAR-1 activation, which is known to rapidly disrupt cell–cell junctions and reduce endothelial monolayer resistance. This reduction in resistance is followed by a recovery period to restore barrier integrity (van Hinsbergh and van Nieuw Amerongen, 2002; Mehta and Malik, 2006). During the recovery phase, tyrosine phosphorylation levels of SHP2 were increased, specifically at tyrosine residue 542. SHP2

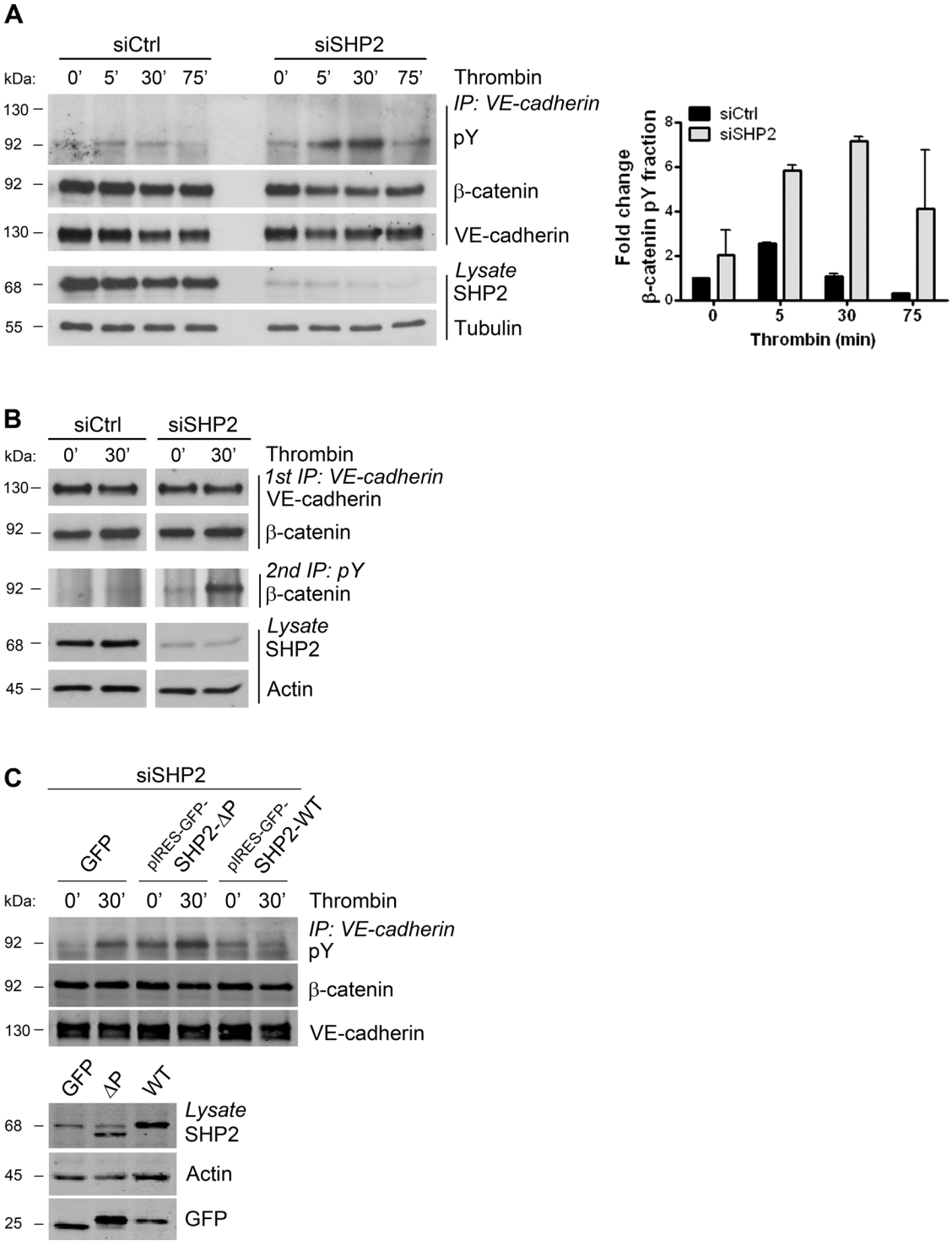

FIGURE 4: Silencing of SHP2 results in prolonged phosphorylation of VE-cadherin–associated β-catenin after thrombin. (A) HUVECs were transfected with control or SHP2 siRNA, grown to confluency, and stimulated with thrombin, as indicated. Cells were lysed, and an IP for VE-cadherin was performed. Phosphorylation levels of the VE-cadherin complex were determined by Western blotting with an anti-phosphotyrosine (pY) antibody. Blot shows prolonged and elevated tyrosine phosphorylation of a VE-cadherin–associating protein of ~92 kDa (likely β-catenin) in SHP2-silenced endothelial monolayers compared with controls. Bar graph, fold increase in tyrosine phosphorylation relative to the levels of VE-cadherin–associating β-catenin. (B) VE-cadherin was immunoprecipitated from cells treated as indicated (top panel; 1st IP: VE-cadherin). From this IP, tyrosine-phosphorylated proteins were immunoprecipitated (third panel; 2nd IP: pY) and analyzed by Western blotting. Top two blots, IP for VE-cadherin with equal levels of β-catenin associating with VE-cadherin during thrombin stimulation. Middle blot, increased phosphorylation of VE-cadherin–associated β-catenin in SHP2-depleted endothelial cells after 30 min of thrombin stimulation compared with controls. Bottom two blots, the protein expression levels of SHP2 and actin in total cell lysates. (C) HUVECs were treated with SHP2 siRNA and 2 d later

phosphorylation at C-terminal tyrosine residues 542 and 580 has been demonstrated to promote SHP2 activation (Lu *et al.*, 2001; Araki *et al.*, 2003) and to occur in an ordered manner, with Tyr-542 phosphorylation preceding phosphorylation of Tyr-580 (Araki *et al.*, 2003). Based on the use of protein ligation techniques to introduce a phosphonate at either Tyr-542 or Tyr-580 of SHP2 and the use of phospho-mutants, phosphorylation of the C-terminal tyrosine residues of SHP2 was shown to be important for SHP2 activity (Lu *et al.*, 2001; Araki *et al.*, 2003). Our data show that increased SHP2 phosphorylation upon thrombin stimulation was induced concomitant with Src-mediated SHP2 activation. Moreover, SHP2 activation occurred in parallel with dephosphorylation of β-catenin. Silencing or inhibition of SHP2 prolonged tyrosine phosphorylation of VE-cadherin–associated β-catenin upon thrombin stimulation, underscoring the specific role for SHP2 in this pathway.

Tyrosine phosphorylation of β-catenin was demonstrated in numerous studies to correlate with a loss of cadherin-adhesive function (Roura *et al.*, 1999; Lilien and Balsamo, 2005; Winter *et al.*, 2008; Monaghan-Benson and Burridge, 2009). However, the molecular basis of this phenomenon is a matter of debate. Several studies described the dissociation of β-catenin from the respective cadherin as a central step in regulating adhesion—for example, after VEGF-induced increases in tyrosine phosphorylation (Monaghan-Benson and Burridge, 2009). This catenin–cadherin dissociation is believed to result in loss of the connection of the cadherin with the actin cytoskeleton, resulting in the disruption of cell–cell adhesion. However, our data show that upon thrombin stimulation, the phosphorylated cadherin–catenin complex remained intact during disruption and reassembly of endothelial cell–cell junctions. Even vanadate-induced tyrosine phosphorylation of junctional proteins did not result in loss of the catenin–cadherin interaction, which is in line with a study of Lampugnani *et al.* (1997). Disassembly of the cadherin–catenin complex was also not observed when increased tyrosine phosphorylation of junctional proteins was induced by leukocyte adhesion to the endothelium (Turowski *et al.*, 2008). Thus complex disassembly does not always follow tyrosine phosphorylation. Different mechanisms may be involved, depending on the stimulus and cell type used. However, tyrosine phosphorylation of junctional proteins and adherens junction disassembly are clearly linked, indicating that dephosphorylation of junctional proteins is likely to be involved in the reassembly of adherens junctions.

However, given that adherens junction composition is not altered upon thrombin stimulation, how does β-catenin dephosphorylation by SHP2 then affect VE-cadherin function? To further study the potential mechanism, we examined whether SHP2 depletion affected the dynamics of VE-cadherin in the plasma membrane. We focused on VE-cadherin dynamics because VE-cadherin is critical for cell–cell adhesion. Of interest, our data showed that silencing of SHP2 reduced the mobility of VE-cadherin in recovering junctions but not in resting cell–cell junctions. In addition, in vanadate-treated cells, the mobile VE-cadherin fraction was reduced, although treatment with vanadate increases tyrosine phosphorylation levels of various proteins besides β-catenin. However, these data indicate that increased tyrosine phosphorylation levels of the cadherin complex prevent proper dynamics that is required for recovery of cell–cell junctions.

Although SHP2 silencing or pharmacological inhibition of SHP2 activity prolonged the thrombin-induced β-catenin phosphorylation and significantly delayed endothelial monolayer recovery, dephosphorylation of β-catenin did occur eventually, accompanied by restoration of the endothelial barrier. This indicates that other adherens junction–associating phosphatases might partially compensate for the absence of SHP2 to restore the restrictive endothelial barrier. Although several phosphatases, including PTP1B, PTPμ, and VE-PTP, promote endothelial barrier function under basal conditions (Nawroth *et al.*, 2002; Sui *et al.*, 2005; Nakamura *et al.*, 2008), the specific role of these phosphatases during junction recovery upon loss of junctional integrity has not been intensively studied. PTP1B associates with VE-cadherin, thereby reducing its tyrosine phosphorylation (Nakamura *et al.*, 2008). In neuronal cells, PTP1B controls cadherin function by dephosphorylating β-catenin, indicating that β-catenin might also be a substrate for PTP1B in endothelial cells (Balsamo *et al.*, 1996). The phosphatase VE-PTP is selectively expressed in endothelial cells and associates with VE-cadherin via its membrane-proximal extracellular domain (Nawroth *et al.*, 2002). The influence of VE-PTP on VE-cadherin function is dependent on plakoglobin, not on β-catenin (Nottebaum *et al.*, 2008). Because plakoglobin associates with VE-cadherin primarily in mature cell–cell junctions in confluent endothelial monolayers (Lampugnani *et al.*, 1995), dephosphorylation of plakoglobin may be less relevant during junction recovery.

Besides dephosphorylation of junctional proteins, several other pathways are important to rapidly restore endothelial barrier function upon thrombin challenge. Activities of the Rho-GTPases Rac1, RhoA, and Cdc42 affect barrier restoration after thrombin (Kouklis *et al.*, 2004; Beckers *et al.*, 2010). Because several studies described a link between SHP2 and Rac1, RhoA, and Cdc42 (Schoenwaelder *et al.*, 2000; Lacalle *et al.*, 2002; Kontaridis *et al.*, 2004; Bregeon *et al.*, 2009; Wang *et al.*, 2009), we tested whether SHP2 silencing affected Rho-GTPase activity upon thrombin stimulation. Our data indicate that SHP2 affects endothelial monolayer recovery independent of Rac1, RhoA, and Cdc42. Nevertheless, the data do not exclude that SHP2 can act downstream of these Rho-GTPases.

Of interest, we observed that SHP2-depleted endothelial monolayers exhibited a prolonged reduction in resistance when challenged by thrombin, whereas the monolayer resistance at baseline or the maximal reduction in resistance in response to thrombin was similar in SHP2-depleted and control monolayers. A possible explanation may be that the formation of new junctions and the reassembly of junctions are two differentially regulated processes. However, a recent study showed that under basal conditions, interference with SHP2 function using the chemical inhibitor NSC-87877 resulted in increased permeability of pulmonary artery endothelial cell monolayers and promoted edema formation in rat lungs (Grinnell *et al.*, 2010). This suggests that SHP2 in pulmonary artery endothelial cell is required for regulation of basal integrity. These discrepancies may be explained by different endothelial cell types used.

Our data showed that β-catenin not only associates with SHP2, but is also a substrate for SHP2. Ukropec *et al.* (2000) demonstrated that thrombin stimulation induced the dissociation of SHP2 from the

infected with adenovirus containing pIRES-GFP-SHP2-WT or a phosphatase domain–deleted mutant (ΔP). HUVECs were stimulated for 30 min with thrombin, and VE-cadherin was immunoprecipitated and immunoblotted with a phosphotyrosine antibody. Reconstitution of SHP-WT rescued β-catenin dephosphorylation, whereas SHP2-ΔP did not. Because a pIRES-GFP vector is used, GFP is not fused to SHP2, and pIRES-GFP runs slightly higher than GFP.

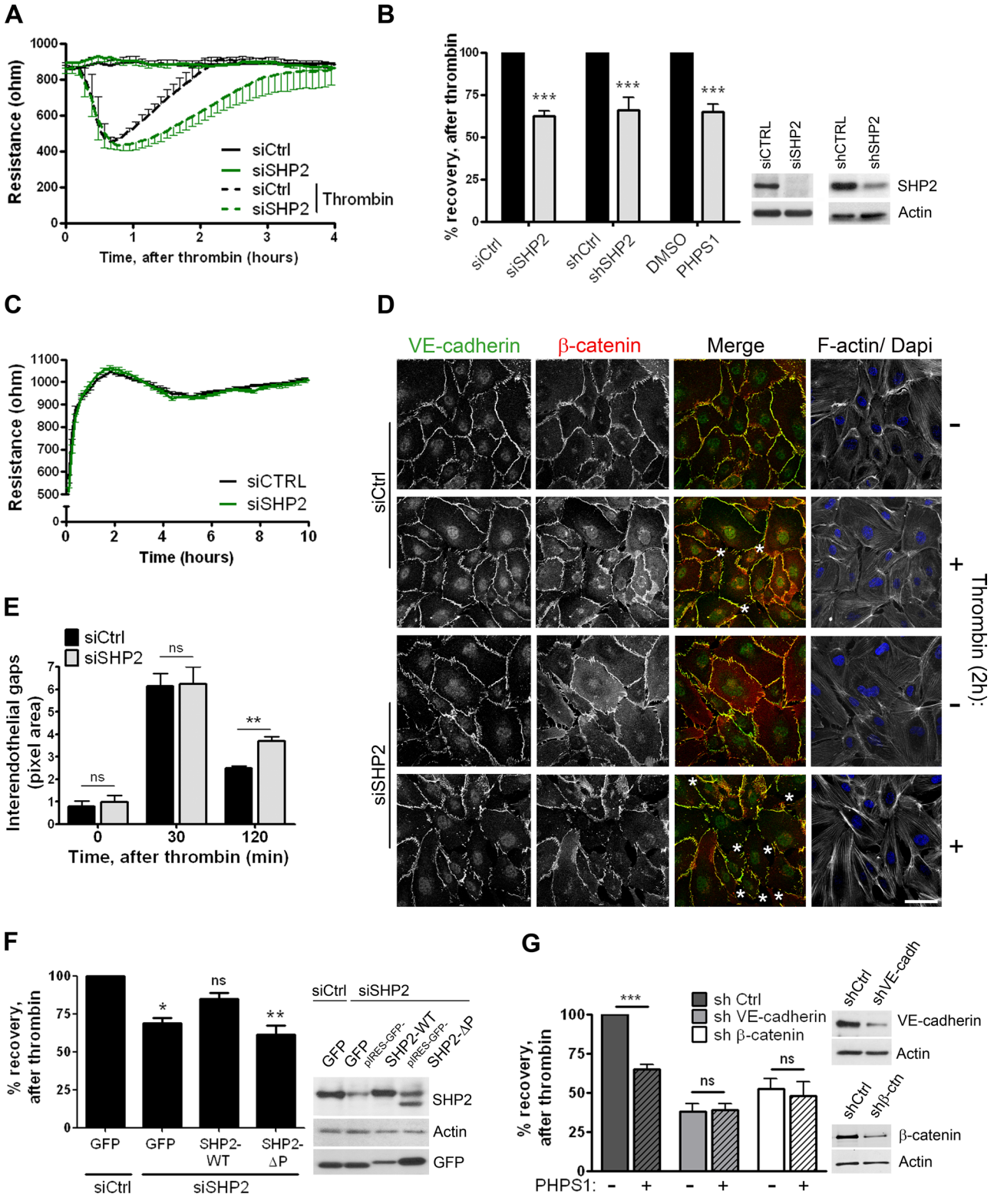

FIGURE 5: SHP2 silencing and inhibition results in delayed cell–cell junction recovery after thrombin stimulation. (A) HUVECs were transfected with control (dark line) or SHP2 (green line) siRNA and grown to confluency on FN-coated electrode arrays. At time point 0, cells were incubated with (dashed line) or without (solid line) thrombin, and the electrical resistance was monitored in time by ECIS. Reduced SHP2 expression resulted in a delayed restoration of the endothelial monolayer TER after thrombin treatment. Representative graph is shown from one of five separate experiments, which were performed in quadruplicate. (B) HUVECs treated with SHP2 siRNA, shRNA, or SHP2 inhibitor PHPS1 were cultured on FN-coated ECIS electrode arrays and stimulated with thrombin. Bar graph, the percentage recovery of the endothelial monolayer resistance after thrombin at time points when control monolayers were completely restored. Both SHP2 silencing and SHP2 inhibition reduced recovery of the endothelial monolayer

VE-cadherin complex, an event that correlated with the increased tyrosine phosphorylation of catenins. Lee *et al.* (2011) suggested that the VE-cadherin complex/SHP2 interaction might be involved in junction restoration not only after thrombin stimulation. They demonstrated that under hypoxic/reoxygenation conditions (an in vitro condition mimicking in vivo ischemia/reperfusion injury), increased endothelial permeability correlated with increased tyrosine phosphorylation levels of VE-cadherin. Angiopoietin-1 treatment then reversed the endothelial permeability increase induced by hypoxia/reoxygenation by restoring the binding of SHP2 to the VE-cadherin complex, possibly resulting in dephosphorylation of the complex. The interesting question remains of whether SHP2 is also involved in endothelial junction recovery after treatment with other permeability-increasing stimuli, such as histamine or bradykinin.

In conclusion, our data show that thrombin-induced loss of endothelial integrity is accompanied by tyrosine phosphorylation but not dissociation of VE-cadherin–linked β-catenin. Subsequent reconstitution of the endothelial barrier involves dephosphorylation of VE-cadherin–associated β-catenin by the tyrosine phosphatase SHP2. SHP2 also promotes the mobility of VE-cadherin in the plasma membrane, stimulating the reassembly of adherens junctions, the closure of intercellular gaps, and restoration of endothelial integrity.

MATERIALS AND METHODS

Antibodies

Monoclonal antibodies (mAbs) to β-catenin, p120-catenin, Cdc42 (clone44), and Rac1 were from BD Transduction Laboratories (Amsterdam, Netherlands). mAbs to VE-cadherin (F8), SHP2, and RhoA and polyclonal Abs to β-catenin and α-catenin were purchased from Santa Cruz Biotechnology (Heidelberg, Germany). VE-cadherin mAb 7H1 was from PharMingen (San Diego, CA), and VE-cadherin mAb BV6 was from Millipore (Amsterdam, Netherlands). The polyclonal Ab to VE-cadherin was from Cayman (Ann Arbor, MI). Abs to phosphotyrosine (pY20) were obtained from Zymed Laboratories (San Francisco, CA) and Enzo Life Sciences (Antwerp, Belgium). SHP2 polyclonal and phosphospecific Abs were purchased from R&D (Las Vegas, NV). mAbs to α-tubulin (DM1A) and actin were purchased from Sigma-Aldrich (Zwijndrecht, Netherlands). mAb to Src was from Cell Signaling Technology (Danvers, MA). The polyclonal phosphospecific (pY418) Ab to Src, mAb to myc, Alexa 633–labeled phalloidin, and secondary Alexa-labeled antibodies were from Invitrogen (Bleiswijk, Netherlands). Secondary horseradish peroxidase (HRP)–labeled antibodies for Western blotting were from Pierce (Rockford, IL).

Cell cultures, treatments, and transfections

Human umbilical vein endothelial cells (HUVECs), purchased from Lonza (Walkersville, MD), were cultured on fibronectin (FN)-coated dishes in EGM-2 medium supplemented with SingleQuots (Lonza). HEK293 and COS-7 cells were maintained in Iscove's modified Dulbecco's medium (BioWhittaker, Verviers, Belgium) containing 10% (vol/vol) heat-inactivated fetal calf serum (Invitrogen, Breda, Netherlands), 300 μg/ml glutamine and 100 U/ml penicillin and streptomycin. Cells were cultured at 37°C at 5% CO_2. When indicated, cells were stimulated with 1 U/ml thrombin (Sigma-Aldrich). To inhibit SHP2 activity, cells were pretreated for 20 h at 37°C with the PTP inhibitor V, PHPS1 (15 μM; Hellmuth *et al.*, 2008), purchased from Calbiochem EMD Biosciences (Darmstadt, Germany). To inhibit activity of the Src-family kinases, cells were pretreated for 30 min with 10 μM PP2 (Calbiochem) or SU6656 (Calbiochem).

SHP2 siRNA (sc-36488-SH) was obtained from Santa Cruz Biotechnology. As a nonspecific control, a siRNA against a luciferase reporter gene was used: CGUACGCGGAAUACUUCGA (5′–3′; Eurogentec, Maastricht, Netherlands). Transfections of siRNA were performed with INTERFERin (Polyplus-transfection, Illkirch, France) according to the manufacturer's recommendations. Cos-7 cells were transiently transfected with the expression vectors indicated in each experiment according to the manufacturer's protocol with Trans IT-LT1 reagent (Myrus, Madison, WI). Myc-tagged pIRES-GFP-SHP WT and catalytic inactive substrate-trapping variants of SHP2, C459S (CS), and D425A (DA) have been previously described (Kolli *et al.*, 2004). After 16–24 h, medium was replaced, and after 2–3 d, cells were used for assays.

Adenovirus containing the C-terminal GFP-tagged VE-cadherin construct was generated as described previously (Allingham *et al.*, 2007). pIRES-GFP-SHP2 WT and phosphatase domain–deleted (ΔP) adenoviruses were generated as described previously (Kontaridis

resistance. Data are mean ± SD of at least two independent experiments, which were performed in duplicate. Blot shows efficient SHP2 protein expression reduction in HUVECs that are transfected or transduced with either siRNA or shRNA against SHP2. (C) Cell spreading and monolayer formation of control and SHP2-depleted endothelial cells, analyzed by ECIS. Experiment was performed as described in A, except that the electrical resistance was monitored directly after cell seeding in serum-free medium. No difference in the electrical resistance during cell spreading and monolayer formation was measured between control and SHP2-deficient endothelial cells. Representative image is shown from one of four separate experiments, which were performed in quadruplicate. (D) HUVECs were grown on FN-coated glass covers, stimulated with thrombin for 2 h or left untreated, processed, and stained for VE-cadherin (green in merged image), β-catenin (red in merged image), and F-actin. Analysis of confocal image shows more interendothelial gaps (asterisks) in SHP2-depleted endothelial monolayers after 2 h of thrombin stimulation. Bar, 20 μm. (E) Quantification of data in D. Analysis of the size of interendothelial gaps showed increased gaps in SHP2-deficient cells 2 h after thrombin treatment. Experiment was carried out three times. Data are mean ± SEM. (F) HUVECs were treated with control or SHP2 siRNA and 2 d later infected with adenovirus containing pIRES-GFP-SHP2-WT or a phosphatase domain–deleted mutant (ΔP). Percentage recovery of the endothelial monolayer resistance after thrombin stimulation was determined as described in B. Reconstitution of SHP_2-WT partially rescued recovery of the endothelial monolayer upon thrombin challenge, whereas SHP2-ΔP did not. Data are mean ± SD of three independent experiments, which were performed in duplicate. (G) VE-cadherin and β-catenin expression was reduced by shRNA. Endothelial cells were grown on FN-coated ECIS electrode arrays and treated with (dashed bars) or without (open bars) the SHP2 inhibitor PHPS1 for 20 h prior to thrombin stimulation. Bar graph shows that the effect of SHP2 inhibition on the restoration of the endothelial monolayer resistance is dependent on the expression of VE-cadherin and β-catenin. Blot shows reduction in VE-cadherin or β-catenin protein expression. Data are mean values of two independent experiments, which were performed in duplicate. ns, not significant; *$p < 0.05$, **$p < 0.01$, ***$p < 0.001$.

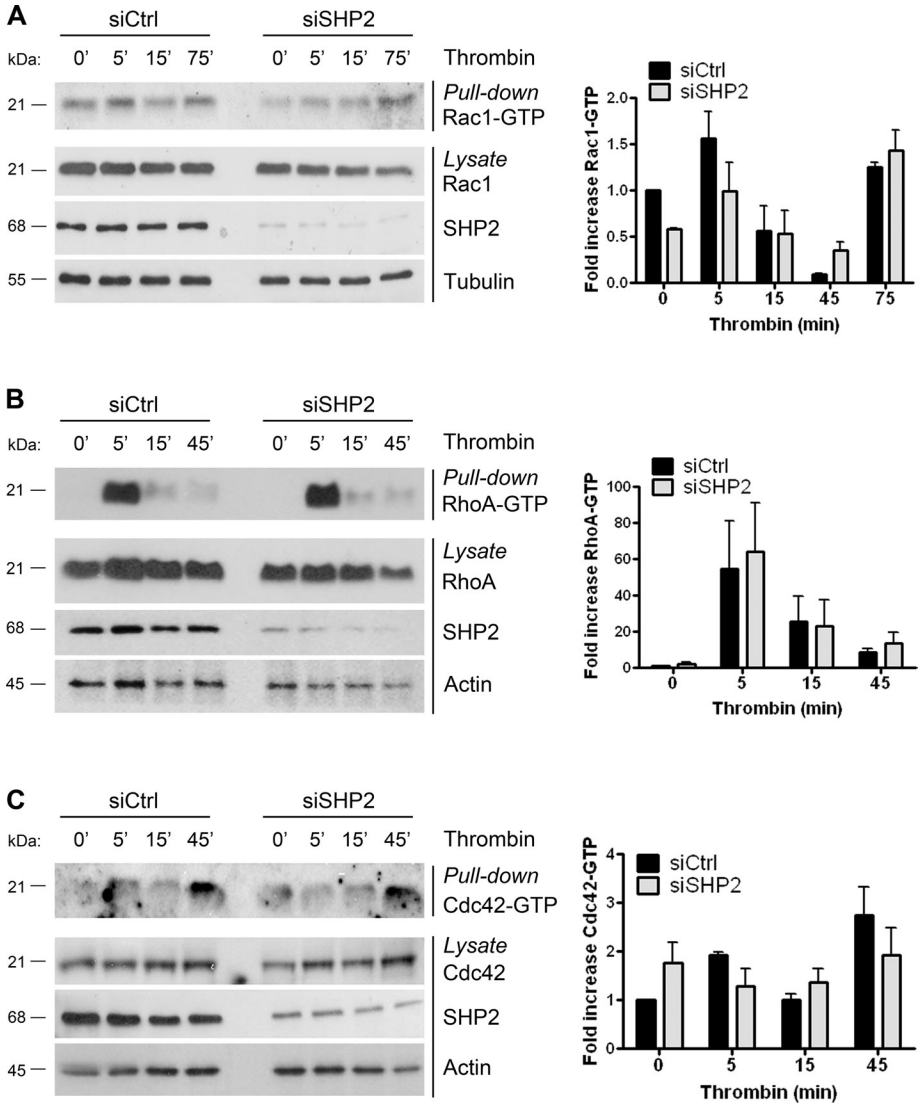

FIGURE 6: Effect of SHP2 silencing on thrombin-induced Rac1, RhoA, and Cdc42 activation. HUVECs were transfected with SHP2 or control siRNA, grown to confluency, and stimulated with thrombin as indicated. (A) Rac1 activation was analyzed using a CRIB-peptide pull-down assay as described in *Materials and Methods* (top). (B) RhoA activation was analyzed using a GST-Rhotekin pull-down assay as described in *Materials and Methods* (top). (C) Cdc42 activation was analyzed using a CRIB-peptide pull-down assay as described in *Materials and Methods* (top). Bottom panels show efficient reduction of SHP2 expression by siRNA and that the expression of Rac1 (A), RhoA (B), Cdc42 (C), and actin or tubulin were equal in total cell lysates. No significant difference in Rac1, RhoA, and Cdc42 activation upon thrombin stimulation was measured in SHP2-deficient cells compared with control cells. Right, the quantification of RhoGTPase activity (GTP levels). Experiments were carried out at least three times.

et al., 2004). One day after infection of cells with the adenovirus, medium was replaced, and after 1 or 2 d of infection, cells were used for assays.

Lentiviral shRNA constructs from the TRC and Sigma Mission library (Root *et al.*, 2006) were obtained from Sigma-Aldrich. The human SHP2-, VE-cadherin-, and β-catenin-specific constructs PTPN11 TRCN_5004, CDH5 TRCN_54090, and CTNNB1 TRCN_3845, respectively, were used. The SHC002 scrambled shRNA construct was used as a negative control. All shRNA constructs were in the pLKO.1 vector backbone. shRNA-expressing lentiviral particles were prepared by transfection of HEK293T cells with the pLKO.1 shRNA plasmid, together with the pMD2.G, pMDLg/RRE, and pRSV-Rev third-generation HIV-1 packaging plasmids (Hope *et al.*, 1990; Dull *et al.*, 1998; obtained from Addgene, Cambridge, MA), using Trans IT-LT1.Virus-containing medium was collected for 3 d posttransfection and cleaned up by filtration through a 0.45-μm polyvinylidene fluoride filter unit (Millipore). Virus was further purified and concentrated by centrifugation for 2 h at 20,000 rpm in a Beckman SW32.1 rotor (Beckman-Coulter, Mijdrecht, Netherlands). Target cells were infected, and 3 d after the addition of virus, cells were used for assays.

Immunoprecipitation and Western blot analysis

A confluent monolayer of cells in a 100-mm dish was washed with ice-cold phosphate-buffered saline (PBS) containing 1 mM $CaCl_2$ and 0.5 mM $MgCl_2$ and lysed in cold NP-40 lysis buffer (25 mM Tris, 100 mM NaCl, 10 mM $MgCl_2$, 10% [vol/vol] glycerol, and 1% [vol/vol] Nonidet P-40, pH 7.4) supplemented with a phosphatase inhibitor cocktail (Sigma-Aldrich) and fresh protease-inhibitor-mixture tablets (Roche, Indianapolis, IN). In some experiments, when studying the VE-cadherin/catenin interaction upon thrombin stimulation, cells were lysed in RIPA lysis buffer (50 mM Tris, 150 mM NaCl, 10 mM $MgCl_2$, 1% [vol/vol] Triton X-100, 0.1% [wt/vol] SDS, and 0.25% [wt/vol] deoxycholic acid). After 10 min of incubation on ice, cell lysates were collected and centrifuged at 10,000 rpm for 10 min at 4°C. The supernatant was incubated with 0.5 μg of mAb to VE-cadherin (BV6; Millipore), 1 μg of mAb to phosphotyrosine (Enzo Life Sciences), or 2 μg of mAb to SHP2 (Santa Cruz Biotechnology) and 50 μl of protein G–Sepharose for 1 h at 4°C under continuous mixing. Subsequently beads were centrifuged at 5000 rpm for 20 s at 4°C, washed five times with lysis buffer, and boiled in SDS-sample buffer containing 4% β-mercaptoethanol. Sequential immunoprecipitations (IPs) for analysis of tyrosine phosphorylation of β-catenin associated with VE-cadherin were performed as described previously (Ukropec *et al.*, 2002). After the first IP, the washed pellet was resuspended in lysis buffer containing 1% SDS. These supernatants were recovered and subjected to a second immunoprecipitation using pY Abs to precipitate tyrosine-phosphorylated proteins from the dissociated VE-cadherin complex.

Samples were then analyzed by SDS–PAGE. Proteins were transferred to a 0.2-μm nitrocellulose membrane (Whatman, Dassel, Germany), which was subsequently blocked with blocking buffer containing 5% (wt/vol) milk powder in Tris-buffered saline with Tween 20 (TBST). When phosphospecific antibodies were used, blots were blocked with 5% (wt/vol) bovine serum albumin (BSA) in TBST. The nitrocellulose membrane was incubated with specific

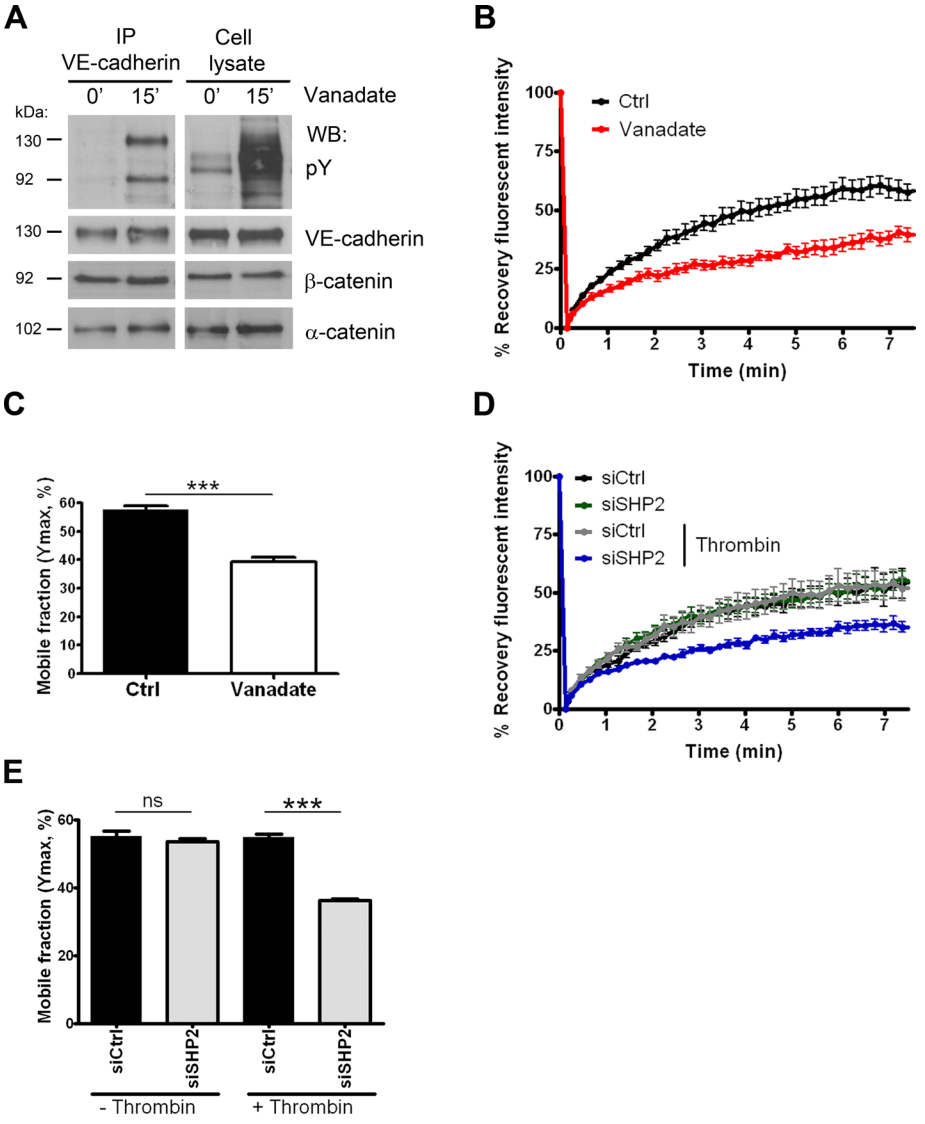

FIGURE 7: Silencing of SHP2 reduces the mobility of VE-cadherin at recovering junctions. (A) HUVECs were treated with 25 μM vanadate and lysed, and an IP for VE-cadherin was performed. Top left, increased tyrosine phosphorylation (pY) of the VE-cadherin complex after vanadate treatment. Bottom panels, staining for β-catenin and α-catenin. (B) FRAP analysis in combination with confocal imaging was used to study the dynamics of VE-cadherin–GFP in HUVECs treated with (red line) or without (dark line) vanadate. Prebleaching intensity was set at 100%. FRAP of VE-cadherin–GFP was reduced when cells were treated with vanadate. (C) Mobile fractions of VE-cadherin–GFP in control and vanadate-treated cells. (D) FRAP analysis of HUVECs transfected with control or SHP2 siRNA, which were stimulated with or without thrombin. The fluorescence recovery of VE-cadherin–GFP in SHP2-depleted cells was only reduced at recovering junctions after thrombin treatment. (E) Mobile fractions are calculated and show that SHP2 depletion reduces the mobile fraction of VE-cadherin–GFP at recovering junctions after thrombin stimulation. Experiments are carried out at least six times, and data are mean ± SEM. ns, not significant; ***$p < 0.001$.

primary antibodies overnight at 4°C, followed by incubation with secondary HRP-labeled antibodies for 1 h at room temperature. Between the incubation steps, blots were washed with TBST. Staining was visualized with an enhanced chemiluminescence detection system (Pierce, Rockford, IL).

SHP2 substrate trapping and GST affinity precipitations

Cos-7 cells transfected with β-catenin and pIRES-GFP-SHP2-myc WT or the substrate-trapping DA and CS mutants were lysed in NP40 lysis buffer and immunoprecipitated for SHP2 by using anti-myc antibodies. For vanadate competition experiments, 10 mM Na_3VO_4 was added. For in vitro substrate trapping, GST-fusion proteins of the SHP2 PTP domain (amino acids 218–528) were used, which were generated as described previously (Kontaridis *et al.*, 2004). The substrate-trapping variant of SHP2, GST-SHP2-DA, contains a mutation at Asp-425 to Ala-425. GST-fusion proteins were purified from BL21 *Escherichia coli* cells (Agilent Technologies, Amstelveen, Netherlands) with glutathione–Sepharose 4B as previously described (Ellerbroek *et al.*, 2004). Cos-7 cells were stimulated with 1 mM vanadate for 30 min and lysed in lysis buffer containing 20 mM Tris, pH 7.5, 100 mM NaCl, 1 mM EDTA, 10% (vol/vol) glycerol, 1% (vol/vol) Triton X-100, and 5 mM iodoacetic acid. After centrifugation at 10,000 rpm for 10 min at 4°C, supernatants were neutralized of iodoacetic acid by incubation with 10 mM dithiothreitol (DTT) and then incubated with GST-empty vector, GST-SHP2-WT, or GST-SHP2-DA for 3 h at 4°C. Finally, in both assays, affinity complexes were washed five times with lysis buffer, boiled at 95°C for 5 min in SDS-sample buffer, and separated by SDS–PAGE as described.

Tyrosine phosphatase activity assay

Cells were lysed on ice for 10 min with 1 ml/dish of lysis buffer (150 mm NaCl, 1 mm EDTA, 40 mm Tris-HCl, pH 7.6, 1% [vol/vol] Triton X-100) supplemented with fresh protease-inhibitor-mixture tablets (Roche). SHP2 proteins were immunoprecipitated using magnetic Dynabeads (Invitrogen), and washed three times in lysis buffer and four times in phosphatase assay buffer (25 mM 4-(2-hydroxyethyl)-1-piperazineethanesulfonic acid, pH 7.2, 50 mM NaCl, 2.5 mM EDTA, 2.5 mM DTT). Levels of immunoprecipitated SHP2 were analyzed by Western blotting. The phosphatase reaction was initiated by incubating the immunocomplexes for 15 min at 30°C in the presence of phosphopeptides END(pY)INASL (Daum *et al.*, 1993) and DADE(pY)LIPQQG (Zhang *et al.*, 1993), according to the Promega protocol (Promega, Madison, WI). In some experiments, when in vitro dephosphorylation of β-catenin by SHP2 was studied, tyrosine-phosphorylated β-catenin was immunoprecipitated from vanadate-treated Cos-7 cells and added to the SHP2 immunocomplex. Phosphate release into the supernatant was detected by addition of Malachite green to the supernatant and measurement of absorbance at 620 nm (Promega protocol).

GTPase activity assays

Rac1 and Cdc42 activation was determined by a Cdc42 and Rac1 interacting binding (CRIB)-peptide pull-down approach, as previously

described (Price *et al.*, 2003). Briefly, cells were lysed and incubated with 30 μg of a biotinylated peptide corresponding to the CRIB domain of Pak. Subsequently lysates were cleared at 14,000 × *g* for 10 min, and supernatants were rotated for 1 h in the presence of streptavidin-coated beads (Sigma-Aldrich) at 4°C. For RhoA activity assays, a C21-GST-Rhotekin fusion protein was used (Ren *et al.*, 1999), which was added to the lysates after the centrifugation step. Supernatants were rotated for 30 min with 60 μg of GST-Rhotekin, which was precoupled to glutathione–Sepharose beads (GE Healthcare Bio-Sciences AB, Chalfont St. Giles, United Kingdom). Finally, in both assays, the beads were washed five times with lysis buffer and boiled in SDS-sample buffer. Samples were analyzed by SDS–PAGE as described.

Electric cell-substrate impedance sensing

Monolayer permeability was determined by measuring the electrical resistance using ECIS. Electrode arrays (8W10E; Applied BioPhysics, Troy, NY) were pretreated with 10 mM L-cysteine (Sigma-Aldrich) for 15 min at 37°C, after which they were washed twice with 0.9% NaCl and subsequently were coated with FN (Sigma-Aldrich) in 0.9% NaCl for 1 h at 37°C. Cells were seeded at 100,000 cells per well (0.8 cm^2) and grown to confluency. Electrical resistance was continuously measured at 37°C at 5% CO_2 with ECIS Model 9600 Controller (Applied BioPhysics). When the electrical resistance of the endothelial monolayer reached a plateau, 1 U/ml thrombin was added. For ECIS-based cell spreading experiments, the increase in resistance in the first hour directly after cell seeding was used as a measure of cell spreading in real time (ten Klooster *et al.*, 2006).

Confocal laser scanning microscopy

For immunofluorescence, cells were cultured on FN-coated glass coverslips. After treatment, cells were washed in cold PBS containing 1 mM $CaCl_2$ and 0.5 mM $MgCl_2$ and fixed in 4% formaldehyde for 10 min. After fixation, cells were permeabilized in 0.2% (vol/vol) Triton X-100 for 10 min, followed by a blocking step in PBS supplemented with 2% (wt/vol) BSA. Cells were incubated with primary and secondary antibodies and, after each step, washed three times in PBS. Coverslips were mounted with Vectashield (Vector Laboratories, Peterborough, United Kingdom) or Mowiol 4-88 reagent (Calbiochem) on microscope slides. Images were recorded with a Zeiss LSM 510 confocal laser scanning microscope (Carl Zeiss, Jena, Germany).

For live-cell imaging, cells were seeded on 30-mm coverslips and transfected as indicated. Cells were placed in a heating chamber at 37°C and recorded with a confocal microscope (Zeiss LSM510). FRAP experiments were performed using 50 iterations with 488-nm laser illumination at maximum power (25 mW). Fluorescence recovery was measured by time-lapse imaging. Prism 4 (GraphPad Software, La Jolla, CA) was used for statistical analysis and nonlinear regression. A single-exponential association was used for curve fitting: $Y = Y_{max}(1 - \exp(-KX))$, which starts at zero and ascends to Y_{max} with a rate constant K, where Y_{max} represents the mobile fraction and K represents the time characteristic of the curve.

Statistical analysis

Statistical comparisons between experimental groups were performed by Student's *t* test. A two-tailed *p* value of ≤0.05 was considered significant.

ACKNOWLEDGMENTS

This work is supported by the Dutch Heart Foundation (Grant 2005T039), the Netherlands Organisation for Scientific Research Veni (Grant 916.76.053), and the Landsteiner Foundation for Blood Transfusion Research (Projects 0903 and 1028).

REFERENCES

Allingham MJ, van Buul JD, Burridge K (2007). ICAM-1-mediated, Src- and Pyk2-dependent vascular endothelial cadherin tyrosine phosphorylation is required for leukocyte transendothelial migration. J Immunol 179, 4053–4064.

Andriopoulou P, Navarro P, Zanetti A, Lampugnani MG, Dejana E (1999). Histamine induces tyrosine phosphorylation of endothelial cell-to-cell adherens junctions. Arterioscler Thromb Vasc Biol 19, 2286–2297.

Angelini DJ, Hyun SW, Grigoryev DN, Garg P, Gong P, Singh IS, Passaniti A, Hasday JD, Goldblum SE (2006). TNF-alpha increases tyrosine phosphorylation of vascular endothelial cadherin and opens the paracellular pathway through fyn activation in human lung endothelia. Am J Physiol Lung Cell Mol Physiol 291, L1232–L1245.

Araki T, Nawa H, Neel BG (2003). Tyrosyl phosphorylation of Shp2 is required for normal ERK activation in response to some, but not all, growth factors. J Biol Chem 278, 41677–41684.

Balsamo J, Leung T, Ernst H, Zanin MK, Hoffman S, Lilien J (1996). Regulated binding of PTP1B-like phosphatase to N-cadherin: control of cadherin-mediated adhesion by dephosphorylation of beta-catenin. J Cell Biol 134, 801–813.

Beckers CM, van Hinsbergh VW, van Nieuw Amerongen GP (2010). Driving Rho GTPase activity in endothelial cells regulates barrier integrity. Thromb Haemost 103, 40–55.

Bregeon J, Loirand G, Pacaud P, Rolli-Derkinderen M (2009). Angiotensin II induces RhoA activation through SHP2-dependent dephosphorylation of the RhoGAP p190A in vascular smooth muscle cells. Am J Physiol Cell Physiol 297, C1062–C1070.

Breviario F, Caveda L, Corada M, Martin-Padura I, Navarro P, Golay J, Introna M, Gulino D, Lampugnani MG, Dejana E (1995). Functional properties of human vascular endothelial cadherin (7B4/cadherin-5), an endothelium-specific cadherin. Arterioscler. Thromb Vasc Biol 15, 1229–1239.

Crosby CV, Fleming PA, Argraves WS, Corada M, Zanetta L, Dejana E, Drake CJ (2005). VE-cadherin is not required for the formation of nascent blood vessels but acts to prevent their disassembly. Blood 105, 2771–2776.

Daniel JM, Reynolds AB (1997). Tyrosine phosphorylation and cadherin/catenin function. Bioessays 19, 883–891.

Daum G, Solca F, Diltz CD, Zhao Z, Cool DE, Fischer EH (1993). A general peptide substrate for protein tyrosine phosphatases. Anal Biochem 211, 50–54.

Davis MA, Ireton RC, Reynolds AB (2003). A core function for p120-catenin in cadherin turnover. J Cell Biol 163, 525–534.

Dejana E, Orsenigo F, Lampugnani MG (2008). The role of adherens junctions and VE-cadherin in the control of vascular permeability. J Cell Sci 121, 2115–2122.

Dull T, Zufferey R, Kelly M, Mandel RJ, Nguyen M, Trono D, Naldini L (1998). A third-generation lentivirus vector with a conditional packaging system. J Virol 72, 8463–8471.

Ellerbroek SM, Wennerberg K, Arthur WT, Dunty JM, Bowman DR, DeMali KA, Der C, Burridge K (2004). SGEF, a RhoG guanine nucleotide exchange factor that stimulates macropinocytosis. Mol Biol Cell 15, 3309–3319.

Esser S, Lampugnani MG, Corada M, Dejana E, Risau W (1998). Vascular endothelial growth factor induces VE-cadherin tyrosine phosphorylation in endothelial cells. J Cell Sci 111, 1853–1865.

Ferber A, Yaen C, Sarmiento E, Martinez J (2002). An octapeptide in the juxtamembrane domain of VE-cadherin is important for p120ctn binding and cell proliferation. Exp Cell Res 274, 35–44.

Grinnell KL, Casserly B, Harrington EO (2010). Role of protein tyrosine phosphatase SHP2 in barrier function of pulmonary endothelium. Am J Physiol Lung Cell Mol Physiol 298, L361–L370.

Hellmuth K, Grosskopf S, Lum CT, Wurtele M, Roder N, von Kries JP, Rosario M, Rademann J, Birchmeier W (2008). Specific inhibitors of the protein tyrosine phosphatase Shp2 identified by high-throughput docking. Proc Natl Acad Sci USA 105, 7275–7280.

Hope TJ, Huang XJ, McDonald D, Parslow TG (1990). Steroid-receptor fusion of the human immunodeficiency virus type 1 Rev transactivator: mapping cryptic functions of the arginine-rich motif. Proc Natl Acad Sci USA 87, 7787–7791.

Hudry-Clergeon H, Stengel D, Ninio E, Vilgrain I (2005). Platelet-activating factor increases VE-cadherin tyrosine phosphorylation in mouse endothelial cells and its association with the PtdIns3′-kinase. FASEB J 19, 512–520.

Huyer G, Liu S, Kelly J, Moffat J, Payette P, Kennedy B, Tsaprailis G, Gresser MJ, Ramachandran C (1997). Mechanism of inhibition of

protein-tyrosine phosphatases by vanadate and pervanadate. J Biol Chem 272, 843–851.
Kemler R (1993). From cadherins to catenins: cytoplasmic protein interactions and regulation of cell adhesion. Trends Genet 9, 317–321.
Kolli S, Zito CI, Mossink MH, Wiemer EA, Bennett AM (2004). The major vault protein is a novel substrate for the tyrosine phosphatase SHP-2 and scaffold protein in epidermal growth factor signaling. J Biol Chem 279, 29374–29385.
Konstantoulaki M, Kouklis P, Malik AB (2003). Protein kinase C modifications of VE-cadherin, p120, and beta-catenin contribute to endothelial barrier dysregulation induced by thrombin. Am J Physiol Lung Cell Mol Physiol 285, L434–L442.
Kontaridis MI, Eminaga S, Fornaro M, Zito CI, Sordella R, Settleman J, Bennett AM (2004). SHP-2 positively regulates myogenesis by coupling to the Rho GTPase signaling pathway. Mol Cell Biol 24, 5340–5352.
Kouklis P, Konstantoulaki M, Vogel S, Broman M, Malik AB (2004). Cdc42 regulates the restoration of endothelial barrier function. Circ Res 94, 159–166.
Lacalle RA, Mira E, Gomez-Mouton C, Jimenez-Baranda S, Martinez A, Manes S (2002). Specific SHP-2 partitioning in raft domains triggers integrin-mediated signaling via Rho activation. J Cell Biol 157, 277–289.
Lampugnani MG, Corada M, Andriopoulou P, Esser S, Risau W, Dejana E (1997). Cell confluence regulates tyrosine phosphorylation of adherens junction components in endothelial cells. J Cell Sci 110, 2065–2077.
Lampugnani MG, Corada M, Caveda L, Breviario F, Ayalon O, Geiger B, Dejana E (1995). The molecular organization of endothelial cell to cell junctions: differential association of plakoglobin, beta-catenin, and alpha-catenin with vascular endothelial cadherin (VE-cadherin). J Cell Biol 129, 203–217.
Lee SW *et al.* (2011). Angiopoietin-1 protects heart against ischemia/reperfusion injury through VE-cadherin dephosphorylation and myocardiac integrin-beta1/ERK/caspase-9 phosphorylation cascade. Mol Med 17, 1095–1106.
Lilien J, Balsamo J (2005). The regulation of cadherin-mediated adhesion by tyrosine phosphorylation/dephosphorylation of beta-catenin. Curr Opin Cell Biol 17, 459–465.
Lu W, Gong D, Bar-Sagi D, Cole PA (2001). Site-specific incorporation of a phosphotyrosine mimetic reveals a role for tyrosine phosphorylation of SHP-2 in cell signaling. Mol Cell 8, 759–769.
Matsuyoshi N, Toda K, Horiguchi Y, Tanaka T, Nakagawa S, Takeichi M, Imamura S (1997). In vivo evidence of the critical role of cadherin-5 in murine vascular integrity. Proc Assoc Am Physicians 109, 362–371.
Mehta D, Malik AB (2006). Signaling mechanisms regulating endothelial permeability. Physiol Rev 86, 279–367.
Monaghan-Benson E, Burridge K (2009). The regulation of vascular endothelial growth factor-induced microvascular permeability requires Rac and reactive oxygen species. J Biol Chem 284, 25602–25611.
Muller WA (2001). Migration of leukocytes across endothelial junctions: some concepts and controversies. Microcirculation. 8, 181–193.
Nakamura Y *et al.* (2008). Role of protein tyrosine phosphatase 1B in vascular endothelial growth factor signaling and cell-cell adhesions in endothelial cells. Circ Res 102, 1182–1191.
Navarro P, Caveda L, Breviario F, Mandoteanu I, Lampugnani MG, Dejana E (1995). Catenin-dependent and -independent functions of vascular endothelial cadherin. J Biol Chem 270, 30965–30972.
Nawroth R, Poell G, Ranft A, Kloep S, Samulowitz U, Fachinger G, Golding M, Shima DT, Deutsch U, Vestweber D (2002). VE-PTP and VE-cadherin ectodomains interact to facilitate regulation of phosphorylation and cell contacts. EMBO J 21, 4885–4895.
Neel BG, Gu H, Pao L (2003). The 'Shp'ing news: SH2 domain-containing tyrosine phosphatases in cell signaling. Trends Biochem Sci 28, 284–293.
Nottebaum AF *et al.* (2008). VE-PTP maintains the endothelial barrier via plakoglobin and becomes dissociated from VE-cadherin by leukocytes and by VEGF. J Exp Med 205, 2929–2945.
Potter MD, Barbero S, Cheresh DA (2005). Tyrosine phosphorylation of VE-cadherin prevents binding of p120- and beta-catenin and maintains the cellular mesenchymal state. J Biol Chem 280, 31906–31912.
Price LS, Langeslag M, ten Klooster JP, Hordijk PL, Jalink K, Collard JG (2003). Calcium signaling regulates translocation and activation of Rac. J Biol Chem 278, 39413–39421.
Rabiet MJ, Plantier JL, Rival Y, Genoux Y, Lampugnani MG, Dejana E (1996). Thrombin-induced increase in endothelial permeability is associated with changes in cell-to-cell junction organization. Arterioscler Thromb Vasc Biol 16, 488–496.
Ren XD, Kiosses WB, Schwartz MA (1999). Regulation of the small GTP-binding protein Rho by cell adhesion and the cytoskeleton. EMBO J 18, 578–585.
Root DE, Hacohen N, Hahn WC, Lander ES, Sabatini DM (2006). Genome-scale loss-of-function screening with a lentiviral RNAi library. Nat Methods 3, 715–719.
Roura S, Miravet S, Piedra J, García de Herreros A, Duñach M (1999). Regulation of E-cadherin/catenin association by tyrosine phosphorylation. J Biol Chem 274, 36734–36740.
Schoenwaelder SM, Petch LA, Williamson D, Shen R, Feng GS, Burridge K (2000). The protein tyrosine phosphatase Shp-2 regulates RhoA activity. Curr Biol 10, 1523–1526.
Sui XF *et al.* (2005). Receptor protein tyrosine phosphatase micro regulates the paracellular pathway in human lung microvascular endothelia. Am J Pathol 166, 1247–1258.
ten Klooster JP, Jaffer ZM, Chernoff J, Hordijk PL (2006). Targeting and activation of Rac1 are mediated by the exchange factor beta-Pix. J Cell Biol 172, 759–769.
Turowski P *et al.* (2008). Phosphorylation of vascular endothelial cadherin controls lymphocyte emigration. J Cell Sci 121, 29–37.
Ukropec JA, Hollinger MK, Salva SM, Woolkalis MJ (2000). SHP2 association with VE-cadherin complexes in human endothelial cells is regulated by thrombin. J Biol Chem 275, 5983–5986.
Ukropec JA, Hollinger MK, Woolkalis MJ (2002). Regulation of VE-cadherin linkage to the cytoskeleton in endothelial cells exposed to fluid shear stress. Exp Cell Res 273, 240–247.
van Hinsbergh VW, van Nieuw Amerongen G (2002). Intracellular signalling involved in modulating human endothelial barrier function. J Anat 200, 549–560.
Vincent PA, Xiao K, Buckley KM, Kowalczyk AP (2004). VE-cadherin: adhesion at arm's length. Am J Physiol Cell Physiol 286, C987–C997.
Wang D, Paria BC, Zhang Q, Karpurapu M, Li Q, Gerthoffer WT, Nakaoka Y, Rao GN (2009). A role for Gab1/SHP2 in thrombin activation of PAK1: gene transfer of kinase-dead PAK1 inhibits injury-induced restenosis. Circ Res 104, 1066–1075.
Weis SM, Cheresh DA (2005). Pathophysiological consequences of VEGF-induced vascular permeability. Nature 437, 497–504.
Winter MC, Shasby S, Shasby DM (2008). Compromised E-cadherin adhesion and epithelial barrier function with activation of G protein-coupled receptors is rescued by Y-to-F mutations in beta-catenin. Am J Physiol Lung Cell Mol Physiol 294, L442-L448.
Xiao K, Allison DF, Buckley KM, Kottke MD, Vincent PA, Faundez V, Kowalczyk AP (2003). Cellular levels of p120 catenin function as a set point for cadherin expression levels in microvascular endothelial cells. J Cell Biol 163, 535–545.
Xiao K, Garner J, Buckley KM, Vincent PA, Chiasson CM, Dejana E, Faundez V, Kowalczyk AP (2005). p120-Catenin regulates clathrin-dependent endocytosis of VE-cadherin. Mol Biol Cell 16, 5141–5151.
Xiao K, Oas RG, Chiasson CM, Kowalczyk AP (2007). Role of p120-catenin in cadherin trafficking. Biochim Biophys Acta 1773, 8–16.
Young BA *et al.* (2003). Protein tyrosine phosphatase activity regulates endothelial cell-cell interactions, the paracellular pathway, and capillary tube stability. Am J Physiol Lung Cell Mol Physiol 285, L63–L75.
Zhang ZY, Thieme-Sefler AM, MacLean D, McNamara DJ, Dobrusin EM, Sawyer TK, Dixon JE (1993). Substrate specificity of the protein tyrosine phosphatases. Proc Natl Acad Sci USA 90, 4446–4450.